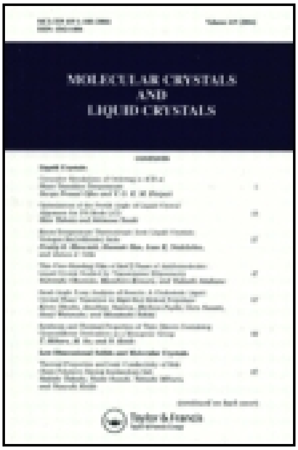

Molecular Crystals and Liquid Crystals Science and Technology. Section A. Molecular Crystals and Liquid Crystals

Publication details, including instructions for authors and subscription information:
http://www.tandfonline.com/loi/gmcl19

Classification of Static Field Effects in Smectic A Mesophase

Vladimir A. Konoplev [a], Dmitry E. Isaychenko [a] & Vladimir K. Pershin [b]

[a] Ural State Technical University, Ekaterinburg, 620002, RUSSIA

[b] Ural State Economical University, Ekaterinburg, 620062, RUSSIA

Version of record first published: 24 Sep 2006

To cite this article: Vladimir A. Konoplev, Dmitry E. Isaychenko & Vladimir K. Pershin (1999): Classification of Static Field Effects in Smectic A Mesophase, Molecular Crystals and Liquid Crystals Science and Technology. Section A. Molecular Crystals and Liquid Crystals, 330:1, 307-325

To link to this article: http://dx.doi.org/10.1080/10587259908025605

Mol. Cryst. Liq. Cryst., 1999, Vol. 330, pp. 307-325
Reprints available directly from the publisher
Photocopying permitted by license only

Classification of Static Field Effects in Smectic A Mesophase

VLADIMIR A. KONOPLEV[a], DMITRY E. ISAYCHENKO[a] and VLADIMIR K. PERSHIN[b]

[a]*Ural State Technical University, Ekaterinburg 620002, RUSSIA and* [b]*Ural State Economical University, Ekaterinburg 620062, RUSSIA*

Bifurcational analysis of the extended Landau-de Gennes model of smectic A (A) liquid crystal in external field is performed. Topological classification of phase diagrams of the system in "field-temperature" coordinates is made. Depending on mesogeneous properties the following static field effects are demonstrated to realize: a) suppression of the nematic (N)-paranematic (pN) phase transition in the critical end point (CEP) (the Wojtowich-Sheng effect) ; b) induction of an intermediate nematic phase (the Rosenblatt effect) followed by its suppression (the induced Wojtowich-Sheng effect); c) induction of tricritical point (TCP) on the A-N phase transition line (the Rosenblatt-Hama effect); d) induction of the A-nonspontaneous nematic (NSN) TCP in combination with the induced Wojtowich-Sheng effect; e) induction of the A-pN TCP in combination with the induced Wojtowich-Sheng effect (the Lelidis-Durand effect); f) induction of the A-NSN-pN triple point (TP) by an arbitrary weak field; g) coincidence of the A-NSN-pN TP and the A-NSN TCP under the influence of the field (field analogue of the Achard-Sigaud-Hardouin effect); h) realization of the A-pN TCP in combination with prohibition of the induced Wojtowich-Sheng effect. Conditions are formulated leading to realization and prohibition of effects listed above.

Keywords: static field effects; phase diagrams

INTRODUCTION

Liquid crystals are extremely sensitive to the action of magnetic and electric fields. A large number of investigations are devoted to description of structural transformations in mesomorphic systems under the influence of external fields. In particular, the orientational order is found to be induced in isotropic–liquid (I) phase as the field is applied; as a result the paranematic (pN) phase occurs. It is predicted theoretically[1-3] that the nematic (N) – pN phase transition occurs without changing of mesophase symmetry, and the phase diagram includes the first–order phase transition line with critical end point (CEP) in "field–temperature" coordinates (the Wojtowich–Sheng effect). Experiments[4] confirmed existing of CEP, but this confirmation was obtained at the limit of experimental resolution regarding the magnitude of electric field applied.

Nematic phase induction (the Rosenblatt effect) was predicted[5] to be possible under the field with intensity comparable to the critical field of the Wojtowich-Sheng effect. In so doing, Rosenblatt[5] considered that in absence of the field the smectic A (A) – isotropic liquid (I) phase transition took place and the smectic A – nonspontaneous nematic (NSN) phase transition was the first order one. In addition, the problem regarding the possibility of tricritical point (TCP) induction on the A–N phase transition line was discussed theoretically[6,7] and the conclusion was made that this effect (the Rosenblatt–Hama one) could be exhibited experimentally under the action of a strong field only.

It has taken near three decades to verify theoretical predictions[1-3,5-7] in experiment[8,9]. In particular, CEP was shown[8] to be reached on the N–pN phase transition line in 4–n–pentyl–4–cyanobiphenyl with large positive dielectric anisotropy under the field of the order of $1{,}4 \cdot 10^5$ V/sm. Similar, but other result, was obtained in more recent paper[9]: CEP on the NSN–pN line (the induced Wojtowich–Sheng effect) was found in 4–n–octyl–cyanobiphenyl and 4'–n–decyl–cyanobiphenyl mixture. Moreover, it was shown[9] that TCP was exhibited on the A–NSN line under more stronger field than it was needed for the NSN–pN CEP realization (the Lelidis–Durand effect). The latter is similar to the effect predicted in the Rosenblatt and Hama theories.

Hence, theoretical investigations[1–3, 5–7] performed describe qualitatively well experimental pattern of phase transformations in smectic A under the field. However, a number of problems remains calling for further discussion and being under investigation in the current paper. Firstly, fundamental problem is not understood from theoretical point of view: is it always possible to induce intermediate nematic phase by the field and does its usual absence in experiment (and therefore, absence of both the Rosenblatt effect and the induced Wojtowich–Sheng one) suggest only about experimental difficulties of generation of required magnitude of the field applied? Secondly, the Rosenblatt–Hama and the Lelidis–Durand effects, while are similar, are different actually: in the first one induction of TCP is predicted on the A–N line, in the latter TCP is observed on the A–NSN line. Therefore, question on the possibility of description of both effects in the frame of unified theory is appropriate. Furthermore, one must not rule out that in some mesogens the A–N and A–NSN phase transitions can occur without TCP formation on relevant phase coexistence lines even under fields as strong as are wished. This assumption requires its confirmation or disproof. Thirdly, it is found[9] that the A–pN TCP realizes at larger field than the NSN–pN CEP. The point is of interest whether this conclusion is inherent to all mesogens with the A–I phase transition in absence of the field or only to specific substances (in particular, the understood ones). In this connection it is also appropriate to recall the paper[10] in which in absence of the field the possibility of coincidence of the A–N–I triple point (TP) and A–N TCP in "concentration–temperature" phase diagram (PD) (the Achard–Sigaud–Hardouin effect) was found. This effect was described theoretically in[11]. Problem under discussion raises the question whether the possibility of field analogy of the Achard–Sigaud–Hardouin effect exists, that is can one find a mesogen or any mixture where coincidence of the A–NSN–pN TP and A–NSN TCP occurs by the field action? Finally, nowadays it is not doubt that one need in very strong fields for observation of the Wojtowich–Sheng effect. Is the analogous conclusion valid for NSN phase formation and realization of both the A–N and A–pN tricritical points under the field?

Problems listed above one can accumulate as the unified problem of classification of static field effects in smectic A mesophase. We consider this problem below on the basis of bifurcational analysis of the Landau–de Gennes model. In the framework of this model all topologically different phase diagrams of mesogens in the "field–temperature" plane are constructed and conditions of realization of the effects under discussion both separately and in combination are found out.

FORMALISM

In accordance with the molecular system symmetry the free energy potential of A mesophase is taken in the form[11, 12]

$$F(Q,S) = \tau_1 Q^2/2 - \beta Q^3/3 + \gamma Q^4/4 + \tau_2 S^2/2 + bS^4/4 - \chi Q S^2 - \mu Q, \quad (1)$$

where β, γ, b, χ are positive material constants; the value $\mu = \chi_a H^2/3$ describes the dimensionless contribution bound up with the action of the external field H; $\chi_a = \chi_{\parallel} - \chi_{\perp} > 0$ is the anisotropy of diamagnetic susceptibility of mesophase molecules; parameters $\tau_k = a_k(T - T_c^k)$, $(a_k > 0,\ k = 1,2)$ characterize deviation of the mesophase temperature T from the lower stability boundary T_c^1 of the I phase and the A–N phase transition temperature T_c^2 in the case when orientational Q and translational S order parameters are non-interacting. From a mathematical point of view the potential (1) corresponds to the truncated modal catastrophe $X_{1,0}$ [11] with two state variables (Q,S) and seven control parameters $\{\tau_1,\tau_2,\beta,b,\gamma,\chi,\mu\}$.

Equations of state of the physical system are determinated from the condition $\nabla F(Q,S) = 0$ and have the form

$$\gamma Q^3 - \beta Q^2 + \tau_1 Q - \mu - \chi S^2 = 0, \tag{2}$$

$$S(\tau_2 - 2\chi Q + bS^2) = 0. \tag{3}$$

Equations (2), (3) describe three types of solutions: S≠0, Q≠0 (A phase), S=0, Q≠0 (N or pN phases), S=0,Q=0 at μ=0 (I phase).

Using Formulae (1)–(3) we can write the stability matrix

$$\mathrm{Hes}(F) = \begin{bmatrix} \tau_1 - 2\beta Q + 3\gamma Q^2 & -2\chi S \\ -2\chi S & \tau_2 - 2\chi Q + 3bS^2 \end{bmatrix}. \tag{4}$$

The zero value of its determinant at the account of solutions (2), (3) defines bifurcational set (separatrix) dividing the control parameters space into open areas with topologically different structures of the potential (1). It is convenient to represent this separatrix as a superposition of three subsets: X_I, ($X'_N \cup X''_N$), and X_A described in (τ_2, τ_1) coordinates, as it is evident from Formulae (2)–(4), by

$$X_I : \tau_1\tau_2 = 0 \tag{5}$$

$$X'_N : \begin{cases} \tau_1 = \beta Q - \gamma Q^2 + \mu / Q, \\ \tau_1 = 2\beta Q - 3\gamma Q^2, \end{cases} \tag{6}$$

$$X''_N : \begin{cases} \tau_1 = \beta Q - \gamma Q^2 + \mu / Q, \\ \tau_2 = 2\chi Q, \end{cases} \tag{7}$$

$$X_A:\begin{cases}\tau_1 = \beta Q - \gamma Q^2 + \mu / Q + \chi F(Q)/Q, & (8)\\ \tau_2 = 2\chi Q - bF(Q), & (9)\\ F(Q) = \left[-2b\gamma Q^3 + b\beta Q^2 + 2\chi^2 Q - b\mu\right]/(b\chi). & (10)\end{cases}$$

Analysis of the curves corresponding to parametric representations (5)–(10) (with Q parameter as the parameter of the curves) allows to provide topological classification of the $X_N^{\prime}, X_N^{\prime\prime}, X_A$ separatrices and phase diagrams in (τ_2,τ_1) and "field–temperature" coordinates and define critical values of the field parameter μ corresponding to different singular points of PD as well.

It follows from Eqs. (7)–(10) that tangency points of the $X_N^{\prime\prime}$ and X_A separatrices obey the equation

$$2b\gamma Q^3 - b\beta Q^2 - 2\chi^2 Q + b\mu = 0. \qquad (11)$$

As it is known[12–17] these points can appear as TCPs in PD of the system under certain conditions. According to (7)–(11) TCP line in (τ_2,τ_1) coordinates is a part of the parabola

$$\tau_1^{TCP} = -3\gamma(\tau_2^{TCP})^2/(4\chi^2) + \tau_2^{TCP}\beta/\chi + 2\chi^2/b$$

with parametric representation

$$\begin{cases}\tau_1 = 2\beta Q - 3\gamma Q^2 + 2\chi^2/b,\\ \tau_2 = 2\chi Q.\end{cases} \qquad (12)$$

Later it will be of interest the right branch of this parabola only (the BB' branch in Figure 1a) when Q parameter in Eq. (12) varies within the range $Q^{B'} \le Q \le Q^B$, where

$$Q^B = (\beta + \sqrt{\beta^2 + 16\chi^2\gamma/b})/(4\gamma), \quad Q^{B'} = \beta/(3\gamma). \qquad (13)$$

Behaviour of smectic A at the left branch of the parabola (12) was investigated in[18, 19].

The A–N–pN TP is determined by equality of free energy minima of these phases

$$F_A(S,Q_A) = F_N(Q_N) = F_{pN}(Q_{pN}) \tag{14}$$

with constraints

$$\nabla F_A(S,Q_A) = 0,\ \nabla F_N(S,Q_N) = 0,\ \nabla F_{pN}(S,Q_{pN}) = 0, \tag{15}$$

where Q_{pN}, Q_N, Q_A are orientational order parameters in corresponding mesomorphic states. This system consists of six equations with respect to unknown values (Q_{pN}, Q_N, Q_A, S, τ_1, τ_2). The result of its solving is detection of the A–N–pN TP line in (τ_2,τ_1) coordinates. Analysis of Eqs. (14)–(15) shows that in the case of strong orientational– translational coupling

$$\chi^2 > b\beta^2/(9\gamma) \tag{16}$$

TP line has the following parametric representation

$$\begin{cases} \tau_1^{TP} = 3\gamma(\mu + 2\mu_{CEP})/\beta, \\ \tau_2^{TP} = 2\chi\beta/(3\gamma) + \sqrt{b\gamma}[\beta^2/(9\gamma^2) + \chi^2/(b\gamma) - 3\mu/\beta] \end{cases} \tag{17}$$

where μ is the parameter of the curve and varies within the range $0 \le \mu \le \mu_{CEP}$; $\mu_{CEP} = \beta^3/(27\gamma^2)$ is the critical field value such that the N–pN phase transition is suppressed, that is the Wojtowich–Sheng effect realizes. Eqs. (17) describe, as well, the A–N–pN TP in the case of compensated orientational–translational coupling

$$\chi^2 = b\beta^2/(9\gamma). \tag{18}$$

However, system behavior changes essentially in the case of weak orientational– translational coupling

$$\chi^2 < b\beta^2/(9\gamma), \tag{19}$$

characterized by the following TP line parametric representation

$$\begin{cases} \tau_1^{TP} = 3\gamma(\mu + 2\mu_{CEP})/\beta, & 0 \le \mu \le \mu_{CEP}, \\ \tau_2^{TP} = \begin{cases} 2\chi\beta/(3\gamma)[1 + \sqrt{1 - \mu/\mu_{CEP}}], & 0 \le \mu \le \mu_{Cr}, \\ 2\chi\beta/(3\gamma) + \sqrt{b\gamma}[\beta^2/(9\gamma^2) + \chi^2/(b\gamma) - 3\mu/\beta], & \mu_{Cr} \le \mu \le \mu_{CEP}, \end{cases} \end{cases} \tag{20}$$

where $\mu_{Cr} = \mu_{CEP}\left[1 - 9\chi^2\gamma/(b\beta^2)\right]$ is the critical field value such that the A–N–pN TP coincides with the A–N TCP. The latter is possible only when the condition (19) is fulfilled; $\mu_{Cr}=0$ when the condition (18) is fulfilled, that is TP coincides with TCP in the absence of the field in (τ_2,τ_1) coordinates; when the condition (16) is fulfilled the A–N TCP realizes already at $\mu=0$ and exists at $\mu>0$ (compare with[11]).

Thus, TP line is the segment of the straight line in the cases of (16), (18), and consists of two pieces — the segment of the straight line (C'C" in Figure 1a) and the part of the parabola (CC' in Figure 1a) joined smoothly at $\mu=\mu_{Cr}$ (in the C' point in Figure 1a) — in the case of (19).

RESULTS AND DISCUSSION

In Figure 1, as an example, it is shown PD in (τ_2,τ_1) plane when the condition (19) is fulfilled ($b=1$, $\beta=1$, $\gamma=1/9$, $\chi=3/4$) and the external field values are different: $0<\mu<\mu_{Cr}$ (Figure 1a), $\mu_{Cr}=\mu_{CEP}$ (Figure 1b), $\mu_{Cr}<\mu\leq\mu_{CEP}$ (Figure 1c). In accordance with Eq. (20) the A–N–pN TP transfers along the CC" curve as μ increases from 0 till μ_{CEP}. As analysis of Eqs. (12) and (20) shows the CC" curve intersects the BB' TCP line in the C' point at $\mu=\mu_{Cr}$ in all relations of model parameters. The areas of localization of two smectic A, A_1, and two nematic N, pN phases are determined by bifurcational set cross–section method[20, 21]. Smectic states evolution under the field was considered in[18, 19] and is not discussed later. First and second order phase transition lines are shown as solid and dotted curves, respectively. The A–N–pN TP lies on the X''_N separatrix at $\mu<\mu_{Cr}$ and in the area between X''_N and X_A curves at $\mu_{Cr}<\mu\leq\mu_{CEP}$.

It is important that if the condition (19) is fulfilled stability areas of A and N states are delimited by the X''_N parabola below the tangency point

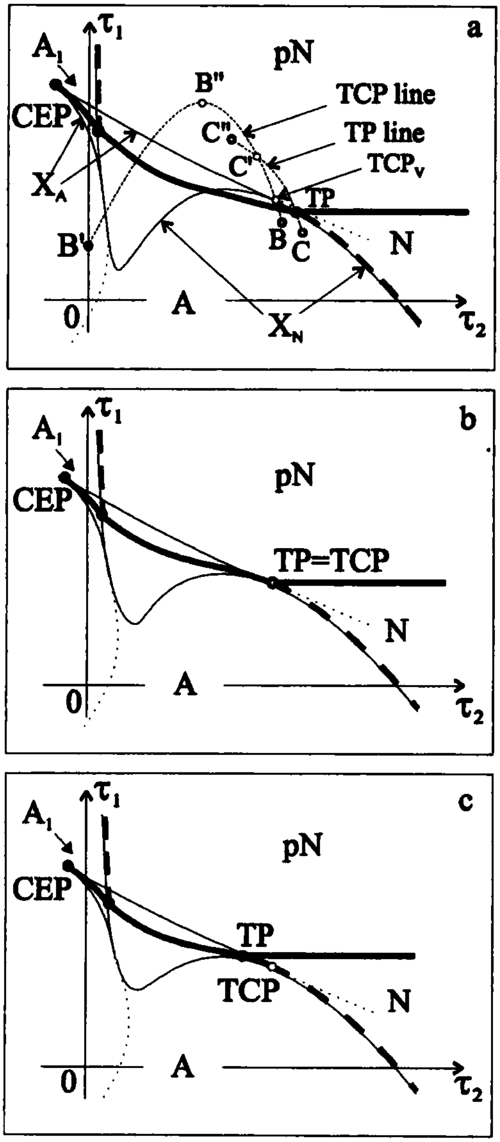

FIGURE 1 Phase diagrams of smectic A liquid crystal in (τ_2,τ_1) coordinates with virtual (a) and real (c) tricritical A-N point and in the case of coincidence of tricritical A-N and triple A-N-I points (b).

(TCP_V in Figure 1a) of the X_A and X_N'' separatrices, and localization areas of A, N and pN states are overlapped above this point. This means that only second order A–N phase transitions are possible below TCP_V point, and only first order ones – above this point; therefore, it can be interpreted as the A–N virtual TCP. However, turning the field on changes PD, "pressing out" the virtual TCP_V (see Figure 1a) into the A and N coexistence area (see Figure 1c). In so doing, at $\mu=\mu_{cr}$ the situation is always available when TCP coincides with TP (see Figure 1b). At $\mu>\mu_{cr}$ the virtual TCP transforms into the real one, the A–N–pN TP leaves the X_N'' separatrix line and moves to the overlapping area of localization region of these three phases.

Different PDs in Figures 1a–c can be represented as the result of deformation of unified PD as μ parameter increases and TP and TCP are displaced along corresponding trajectories CC" and BB'. These phase diagrams can be interpreted as the cross–sections of three–dimensional PD in (τ_2,τ_1,μ) coordinates by μ=const planes, this allows to recalculate (τ_2,τ_1) PDs into "field–temperature" ones. In so doing, one must take into account that, in so far as according to Landau theory of phase transitions thermodynamical evolution of specific mesogen is in conformity with oriented straight line directed from III to I quadrant of (τ_2,τ_1) plane, we can introduce a dimensionless mesophase temperature τ by equations

$$\tau_1 = A\tau + B, \quad \tau_2 = \tau, \tag{21}$$

where A>0 and B are the parameters of thermodynamic way. In so doing, lines (21), at different values of A and B, can be interpreted as thermodynamic ways of mesogens of the same homologous series or mesophase mixture with different component concentration. Results of proper recalculation are presented in Figure 2 (χ=5/4, graphs 1–7) and Figure 3 (χ=3/4, graphs 1–9) at coupling conditions (16), (19). Calculations of (μ,τ) PDs were carried

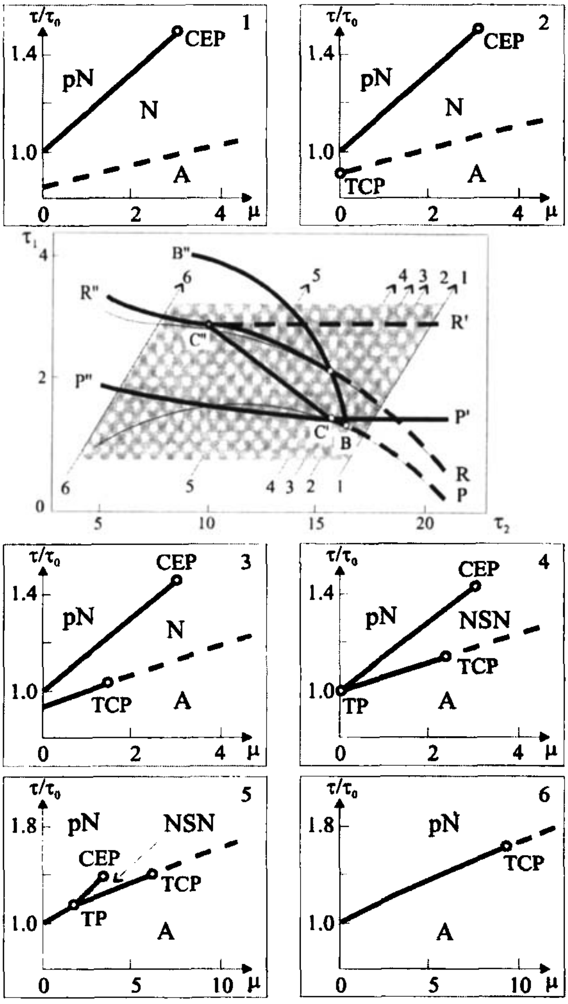

FIGURE 2 Phase diagrams in (τ_2,τ_1) (central part) and (μ,τ) coordinates (graphs 1-6: B=6.5(1),6.0(2),5.5(3),5.2(4),4.0(5),2.8(6);A=0.5)

out for fixed thermodynamic ways shown in the center of these Figures as straight lines against the background of fragments of (τ_2,τ_1) PDs in the vicinity of the A–N–pN TP. As an example, the P–P'–P" and R–R'–R" curves being in conformity with different transition lines at μ=0 and $\mu=\mu_{CEP}$, respectively, are presented in the central parts of Figures 2 and 3 as well. Analysis of possible arrangement of the A–N TCP (12) and the A–N–pN TP (17),(20) curves with respect to thermodynamic ways (21) allows to write the conditions of realization of all field effects described by the model under consideration. The basic analytic results of this analysis performed for cases (16) and (19) separately are presented in Table 1 and numerical ones are in Figures 2 and 3.

Formulae (12), (13), (17), (20), (21) allow to determine field and temperature values such that the A–N TCP and the A–NSN–pN TP are realized in PD. These values are

$$\mu^{TCP} = -2\gamma Q_{TCP}^3 + \beta Q_{TCP}^2 + 2\chi^2 Q_{TCP} / b, \tag{22}$$

$$\tau^{TCP} = 2\chi Q_{TCP}, \tag{23}$$

for TCP, where Q_{TCP} is the greatest positive root of equation

$$3b\gamma Q^2 + 2b(\chi A - \beta)Q + (bB - 2\chi^2) = 0. \tag{24}$$

For TP these values take different forms in accordance with approximation used: in the case of (16)

$$\mu^{TP} = \beta\left\{A\left[b\beta^2 - 9\gamma\chi^2 + 6\beta\chi\sqrt{b\gamma}\right] + \sqrt{b\gamma}(9B\gamma - 2\beta^2)\right\} * \\ *\left[27\gamma^2(b + \sqrt{b\gamma})\right]^{-1}, \tag{25}$$

$$\tau^{TP} = 2\beta\chi/(3\gamma) + \sqrt{b/\gamma}\left[\beta^2/(9\gamma) + \chi^2/b\right] - 3\mu^{TP}\sqrt{b\gamma}/\beta; \tag{26}$$

in the case of (19)

$$\mu^{TP} = \beta\left[-D + \sqrt{D^2 - \gamma^2 G^2 - 4A\beta\chi G/(3\gamma)}\right], \tag{27}$$

$$\tau^{TP} = 2\beta\chi/(3\gamma)\left[1 + \sqrt{1 - \mu_{TP}/\mu_{CEP}}\right], \tag{28}$$

where

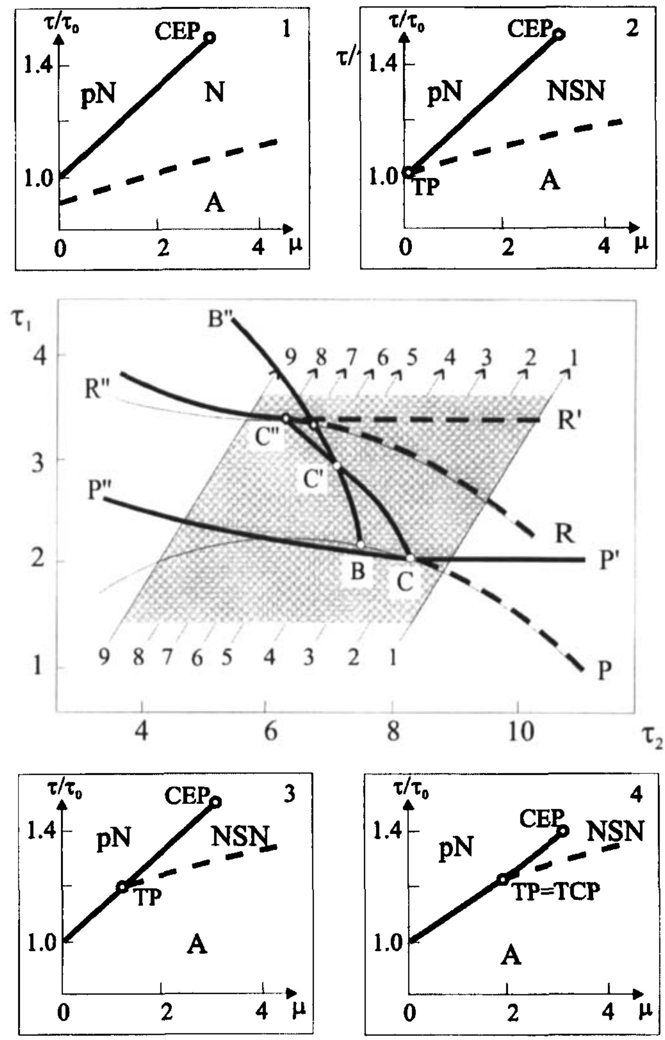

FIGURE 3 Phase diagrams in (τ_2,τ_1) (central part) and (μ,τ) coordinates (graphs 1-10: B=2.7 (1), 2.2 (2), 1.1 (3), 1.0 (4), 0.7 (5), 0.53 (6), 0.3 (7), 0.17 (8), 0.5 (9); A=0.5)

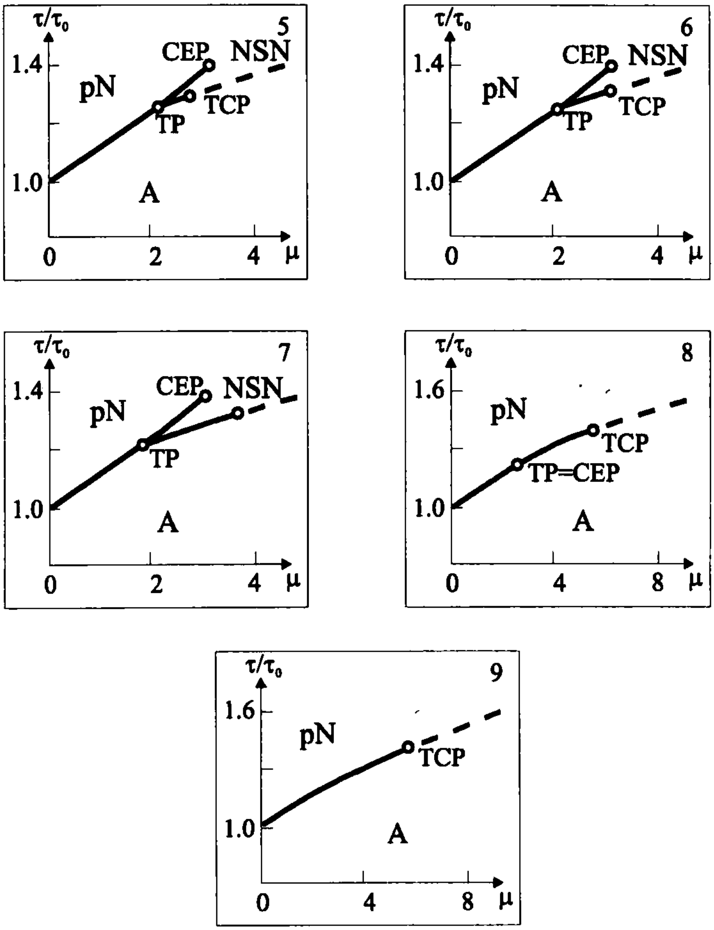

FIGURE 3 Continued

$$G = 6\gamma\mu_{CEP}/\beta - B,\quad D = \gamma[G - 2A\beta\chi/(3\gamma)] + 2A^2\chi^2. \tag{29}$$

Formulae (27)–(29) are valid at the condition $\mu^{TP} \le \mu_{Cr}$. At the opposite condition $\mu_{Cr} < \mu^{TP} \le \mu_{CEP}$ one must use previous Eqs. (25),(26). Note that calcula-

TABLE 1

Effect	Conditions of effect realization in the case	
	$\chi^2 > b\beta^2/(9\gamma)$	$\chi^2 < b\beta^2/(9\gamma)$
The A–N phase transition of second order in arbitrary strong fields (absence of the Rosenblatt effect); the Wojtowich–Sheng effect is available	$B < [\beta + \sqrt{\beta^2 + 16\gamma\chi^2 / b}]* *[4\beta - A\chi]/(8\gamma) - \chi^2/b$	$B < 2\beta[\beta - 6A\chi]/(9\gamma)$
Induction of the A–N TCP by arbitrary weak fields (the Rosenblatt–Hama effect)	$B \geq [\beta + \sqrt{\beta^2 + 16\gamma\chi^2 / b}]* *[4\beta - A\chi]/(8\gamma) - \chi^2/b$, $B < 2[\beta^2 - 3A\beta\chi]/(9\gamma) - A\sqrt{b\gamma}[\beta^2/(9\gamma^2) + \chi^2/(b\gamma)]$	
Mutual induction of an intermediate N phase and the A–N TCP by arbitrary weak fields (conjunction of the Rosenblatt and the Rosenblatt–Hama effects)	$B < [\beta^2 - 2A\beta\chi]/(3\gamma) - A\chi^2/\sqrt{b\gamma}$, $B \geq 2[\beta^2 - 3A\beta\chi]/(9\gamma) - A\sqrt{b\gamma}[\beta^2/(9\gamma^2) + \chi^2/(b\gamma)]$	

TABLE 1 Continued

Induction of an intermediate N phase by arbitrary weak fields in absence of the A–N TCP (realization of the Rosenblatt effect with prohibition of the Rosenblatt–Hama effect)	—	$B \geq 2\beta[\beta - 6A\chi]/(9\gamma)$ $B < \beta^2/(6\gamma) - 3\chi^2/b -$ $- 4A\chi(\beta + 3\chi\sqrt{\gamma/b})/(6\gamma)$
Coincidence of the A–N–pN TP and the A–N TCP by the field (the field analogy of the Achard–Sigaud–Hardouin effect)	—	$B = \beta^2/(6\gamma) - 3\chi^2/b -$ $- 4A\chi(\beta + 3\chi\sqrt{\gamma/b})/(6\gamma)$
Induction of the A–NSN TCP by strong field (the Lelidis–Durand effect)	$B > [\beta^2 - 2A\beta\chi]/(3\gamma) -$ $- A\chi^2/\sqrt{b\gamma}$, $B \leq 2[\beta^2 - 3A\beta\chi]/(9\gamma) -$ $- A\sqrt{b\gamma}[\beta^2/(9\gamma^2) + \chi^2/(b\gamma)]$	$B > \beta^2/(6\gamma) - 3\chi^2/b -$ $- 4A\chi(\beta + 3\chi\sqrt{\gamma/b})/(6\gamma)$ $B \leq [\beta^2 - 2A\beta\chi]/(3\gamma) -$ $- A\chi^2/\sqrt{b\gamma}$,
Coincidence of the A–N–pN TP and the N–pN CEP by field	$B = [\beta^2 - 2A\beta\chi]/(3\gamma) -$ $- A\chi^2/\sqrt{b\gamma}$,	$B = [\beta^2 - 2A\beta\chi]/(3\gamma) -$ $- A\chi^2/\sqrt{b\gamma}$,
Realization of the A–pN TCP without induction of an intermediate N phase	$B > \beta[\beta - 2A\chi]/(3\gamma) -$ $- A\chi^2/\sqrt{b\gamma}$, $B < \beta[\beta - 2A\chi]/(3\gamma) + 2\chi^2/b$	$B > \beta[\beta - 2A\chi]/(3\gamma) -$ $- A\chi^2/\sqrt{b\gamma}$, $B < \beta[\beta - 2A\chi]/(3\gamma) + 2\chi^2/b$

tions by Formulae (22)–(24) lead to accurate results only if the thermodynamical way (21) intersects the TCP line (12) in (τ_2,τ_1) plane. Analogous remark refers to Eqs. (25)–(29), but this case requires the occurrence of a common point of the TP line (17) or (20) and the straight line (21).

In Figure 2 the graph 1 describes the A–N–I phase transitions sequence at μ=0, the A–N–pN sequence in the range $0<\mu<\mu_{CEP}$, during which the A–N PTs are of second order. In graph 2 new feature appears: the A–N TCP originates at μ^{TCP}=0 and exists at μ^{TCP}>0 (see graph 3 also). This means, in contrast to[6,7], that the Landau–de Gennes model predicts the possibility of realization of the Rosenblatt–Hama effect in fields as weak as are wished. Situation when intermediate NSN phase arises in weak fields with concurrent occurrence of TCP on the A–NSN phase transition line is presented in graphs 4 and 5. Anyone of a number of cases is possible: $\mu^{TCP}<\mu_{CEP}$ (graph 4), $\mu^{TCP}=\mu_{CEP}$ and $\mu^{TCP}>\mu_{CEP}$ (graph 5). The latter is in conformity with experimentally observed the Lelidis–Durand effect[9]. Note that $\mu^{TCP}>\mu^{TP}$ always for the case (16). In addition, analysis shows that, if the limiting condition $\chi^2 \to b\beta^2/(9\gamma)$ is fulfilled, induction both the A–NSN–pN TP and the A–NSN TCP occur at $\mu^{TP}<<\mu_{CEP}$, $\mu^{TCP}<<\mu_{CEP}$, that is the Lelidis–Durand effect can be observed not only under strong field but under weak one as well. Besides, there is the possibility of coincidence the A–NSN–pN TP and the NSN–pN CEP at $\mu^{TCP}>\mu^{TP}=\mu_{CEP}$ (not shown in graph). In this case induction and concurrent suppression of intermediate N phase occur. In graph 6 the only effect of the A–pN TCP induction realizes (the Rosenblatt effect is prohibited). This is true under strong field only.

Graphs presented in Figure 3 allow to carry out classification of field effects in smectic A in the case (19). Let us point out some fundamental features only. Firstly, the effect of induction of the A–NSN–pN TP with totally second–order A-NSN boundary is possible (see graphs 2 and 3), that is in this case realization of the Rosenblatt effect at $\mu^{TP}\rightarrow 0$ with prohibition of the Rosenblatt–Hama effect (see line 4 of Table 1) is possible. Secondly, the model leaves room for coincidence of the A–N TCP and the A–N–pN TP at $\mu^{TP}=\mu^{TCP}=\mu_{Cr}$ (see graph 4 and line 5 of Table 1), that is the field analogy of the Achard–Sigaud–Hardouin effect[10] is possible in the approximation (19) only. Realization of some effects is possible in the approximation (16) only (see lines 2 and 3 of Table 1). A number of effects are available in the case of both strong and weak orientational–translational coupling (see lines 1 and 6–8 of Table 1).

CONCLUSION

Thus, we describe the well–known field effects (the Rosenblatt, Rosenblatt–Hama, Lelidis–Durand, Wojtowich–Sheng effects) and predict the novel ones (field analogy of the Achard–Sigaud–Hardouin effect, coincidence of the NSN–pN CEP and the A–NSN–pN TP, realization of the A–N TCP in the absence of intermediate N induction effect). Conditions when a number of effects can be prohibited for realization in certain mesogens and when some of them must be mutually conjugate are determined (see Table 1). Note also that the effect of induction of the N–pN CEP is often lies in the limit of experimental possibilities, whereas the investigation performed allows to conclude that there are no fundamental physics reasons for the A–NSN–pN TP and the A–NSN TCP could not be observed at essentially smaller field values.

Acknowledgments

This work was supported by RBRF Grant. Support received from the Organizing Committee of 16th ILCC, Kent, USA.

References

[1] J. Hanus, *Phys. Rev.*, **178**, 420 (1969).
[2] P.J. Wojtowich, and P. Sheng, *Phys. Lett. A.*, **48**, 235 (1974).
[3] R. Hornreich, *Phys. Lett. A.*, **109**, 232 (1985).
[4] A. Nicastro, and P. Keyes, *Phys. Rev. A.*, **30**, 3156 (1984).
[5] C. Rosenblatt, *Phys. Lett. A.*, **83**, 221 (1981).

[6] C. Rosenblatt, *J. de Phys. Lett.*, **42,** L-9 (1981).
[7] H. Hama, *J. Phys. Soc. Jap.*, **54,** 2204 (1985).
[8] I. Lelidis, and G. Durand, *Phys. Rev. E.*, **48,** 3822 (1993).
[9] I. Lelidis, and G. Durand, *Phys. Rev. Lett.*, **73,** 672 (1994).
[10] M.P. Achard, G. Sigaud, and P. Hardouin, in *Liquid crystals in one and two dimensions*, edited by G.W. Gray (Berlin, 1980), p. 149.
[11] V1.K. Pershin, *Zurnal Phiz. Him.*, **69,** 65 (1995).
[12] P. de Gennes, *The Physics of Liquid Crystals* (Clarendon Press, Oxford, 1974), 444 p.
[13] V1.K. Pershin, and V.A. Konoplev, *Mol. Cryst. Liq. Cryst.*, **192,** 1 (1990).
[14] Vl.K. Pershin, and V.A. Konoplev, *Mol. Cryst. Liq. Cryst.*, **209,** 171 (1991).
[15] V1.K. Pershin, V.A. Konoplev, and D.V. Jukovsky, *Chem. Phys. Lett.*, **186,** 270 (1991).
[16] Vl.K. Pershin, and A.V. Khomenko, *Mol. Cryst. Liq. Cryst.*, **220,** 159 (1992).
[17] V.A. Konoplev, V1.K. Pershin, and R.A. Raevsky, *Mol. Cryst. Liq. Cryst.*, **260,** 531 (1995).
[18] V.A. Konoplev, V1.K. Pershin, and R.A. Raevsky, *Izvestiya RAN*, **61,** 1027 (1997).
[19] V.A. Konoplev et al, *Mol. Cryst. Liq. Cryst.*, **301,** 411 (1997).
[20] V.A. Konoplev, Vl.K. Pershin, and A.V. Khomenko, *Mol. Cryst. Liq. Cryst*, **301,** 31 (1997).
[21] V.A. Konoplev, et al, *Mol. Cryst. Liq. Cryst.*, **299,** 51 (1997).